Graphene radio frequency devices on flexible substrate

Wenjuan Zhu, Damon B. Farmer, Keith A. Jenkins, Bruce Ek, Satoshi Oida, Xuesong Li, Jim Bucchignano, Simon Dawes, Elizabeth A. Duch, and Phaedon Avouris

---

Articles you may be interested in

Spatial/temporal photocurrent and electronic transport in monolayer molybdenum disulfide grown by chemical vapor deposition
Applied Physics Letters **108**, 083104 (2016); 10.1063/1.4942508

Realization of a high mobility dual-gated graphene field-effect transistor with Al_2O_3 dielectric
Applied Physics Letters **94**, 062107 (2009); 10.1063/1.3077021

2D-2D tunneling field-effect transistors using WSe_2/$SnSe_2$ heterostructures
Applied Physics Letters **108**, 083111 (2016); 10.1063/1.4942647

Impact of gate resistance in graphene radio frequency transistors
Applied Physics Letters **101**, 143503 (2012); 10.1063/1.4757422

Contact resistance in few and multilayer graphene devices
Applied Physics Letters **96**, 013512 (2010); 10.1063/1.3290248

High-performance MoS_2 transistors with low-resistance molybdenum contacts
Applied Physics Letters **104**, 093106 (2014); 10.1063/1.4866340

CrossMark
click for updates

Graphene radio frequency devices on flexible substrate

Wenjuan Zhu,[a] Damon B. Farmer, Keith A. Jenkins, Bruce Ek, Satoshi Oida, Xuesong Li, Jim Bucchignano, Simon Dawes, Elizabeth A. Duch, and Phaedon Avouris[b]

IBM Thomas J. Watson Research Center, Yorktown Heights, New York 10598, USA

Graphene is a very promising candidate for applications in flexible electronics due to its high carrier mobility and mechanical flexibility. In this paper, we present results on graphene RF devices fabricated on polyimide substrates with cutoff frequencies as high as 10 GHz. Excellent channel mobility and current saturation are observed in graphene long channel devices on polyimide. Graphene devices on polyimide also show very good temperature stability from 4.4 K to 400 K and excellent mechanical flexibility up to a bending radius of 1 mm. These demonstrated properties make graphene an excellent candidate for flexible wireless applications. © 2013 AIP Publishing LLC. [http://dx.doi.org/10.1063/1.4810008]

Flexible electronics is a rapidly growing field due to its wide range of potential applications, including display technology,[1] wearable electronics,[2] flexible solar cells,[3] e-paper,[4] and bio-medical skin-like devices.[5] In the past, the primary materials for flexible electronics were organic polymers, amorphous silicon,[6] or oxide-based semiconductors.[7] The carrier mobilities in these materials are typically very low, and as such, these materials are only suitable for low-speed applications such as flexible displays, electronic tags, and low-cost integrated circuits.[5,8] High frequency applications such as wireless communications require materials with higher carrier mobility. Recently, thin silicon membranes and III-V membranes transferred to flexible substrates were reported.[9–11] However, due to the brittle nature of the silicon and III-V crystal, the bending radius is limited.

Graphene is an ideal material for flexible applications due to its high carrier mobility, optical transparency, and mechanical flexibility. High-frequency graphene RF devices on rigid substrates have been demonstrated with cut-off frequencies exceeding 300 GHz[12] and subsequently graphene-based circuits have been successfully made.[13,14] By contrast, the device performances of graphene on flexible substrate are lagging behind.[11,15–23] Here, we demonstrate graphene RF devices on flexible polyimide that operate with relatively high cut-off frequencies of 10 GHz, and exhibit both good temperature stability and excellent mechanical flexibility.

A representative schematic of the graphene RF device on polyimide and an optical image of the device array are shown in Figures 1(a) and 1(b), respectively. The growth and transfer of large area graphene was performed using the approaches reported by Li.[24] After graphene formation, PMMA was spin-coated on top of the graphene layer formed on one side of the Cu foil. This Cu foil was then dissolved in copper etchant. The resulting graphene/PMMA layer was transferred to polyimide substrates, and the PMMA was later dissolved in acetone. The polyimide film substrate is 0.127 mm thick. To reduce the surface roughness, liquid polyimide PI-5878G and adhesion promoter VM651 are also

used. Metal electrode deposition was done by electron-beam evaporation at 10^{-7} Torr. 20 nm Pd/30 nm Au stacks were used for the source/drain contacts. The gate oxide is AlOx formed by an oxidized Al layer that was deposited by electron-beam evaporation followed by the deposition of 30 nm HfO$_2$ by atomic layer deposition.

Figures 2(a) and 2(b) show the DC characteristics of a typical long channel device (gate length = 4 μm) with gate width of 1 μm. The Dirac voltage is close to zero ($\sim$0.47 V) and the electron and hole branches are nearly symmetric. This indicates the initial doping of the graphene is very small. The channel mobility is extracted to be about 1830 cm^2/V-s using the drift model.[25] Good drain current saturation, which is typically difficult to obtain in graphene devices, is observed for these devices, as shown in Figure 2(b). The RF performance can be estimated from this DC data. The cutoff frequency, f_T, is estimated from the transconductance, g$_m$, using the equation $f_T = g_m/2\pi C_g$, where C$_g$ is the gate capacitance. In turn, the maximum oscillation frequency, f$_{max}$, can be estimated using the equation:[26] $f_{max} \approx f_T/\sqrt{4g_d(R_s + R_G) + 8\pi C_g R_G f_T}$, where R_s is the series resistance, R_G is the gate resistance, and $g_d = dI_d/dV_d$ is the output conductance. From the DC results in Figure 2, we estimate f_T to be 1.4 GHz and f_{max} to be 10.1 GHz at a gate voltage of V$_g$ = 0 V and a drain bias of V$_d$ = −2 V. Here we use the resistivity of Ti, Pd, and Au of 4.31 × 10^{-5} Ω cm, 1.05 × 10^{-5} Ω cm, 2.2 × 10^{-6} Ω cm,[27] the dielectric constant for AlO$_x$ and HfO$_2$ are 6 and 13, respectively,[25,28] the contact resistivity and access resistivity are 314 Ω μm and 0.04 Ω/nm.[26] Good drain current saturation, i.e., low output conductance, g$_d$, is essential for a high f$_{max}$. For a shorter channel device, the cut-off frequency f$_T$ will increase as the device length L$_g$ reduces ($f_T \propto 1/L_g$) (Ref. 29). However, current saturation is harder to attain due to the influence of contact resistance and short channel effects.[12] As a result, the f$_{max}$ is actually lower for shorter channel devices.

The frequency response of the devices was determined directly through measurements of the scattering (S) parameters of the transistors with a network analyzer. The short-circuit current gain |h21| (the ratio of small-signal drain and gate currents) is obtained from the measured S-parameters,

[a]wenjuan@us.ibm.com
[b]avouris@us.ibm.com

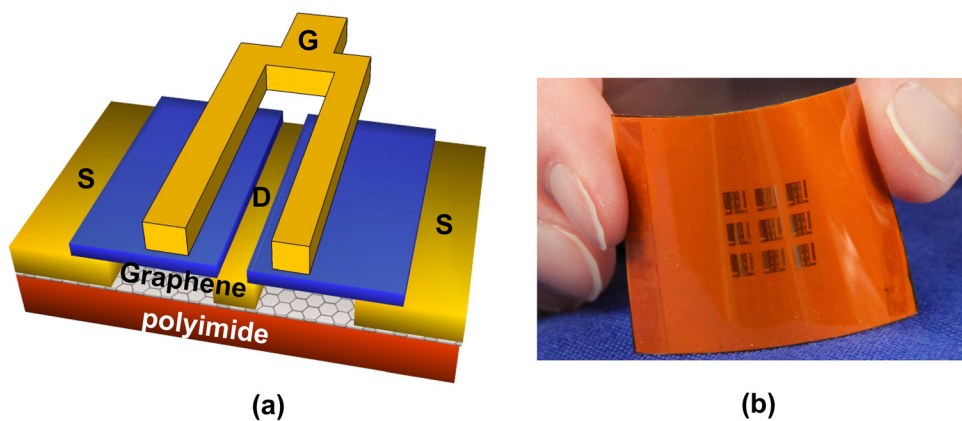**(a)**   **(b)**

FIG. 1. (a) Schematic of the graphene RF device on polyimide. (b) Optical image of a graphene device array on the polyimide substrate.
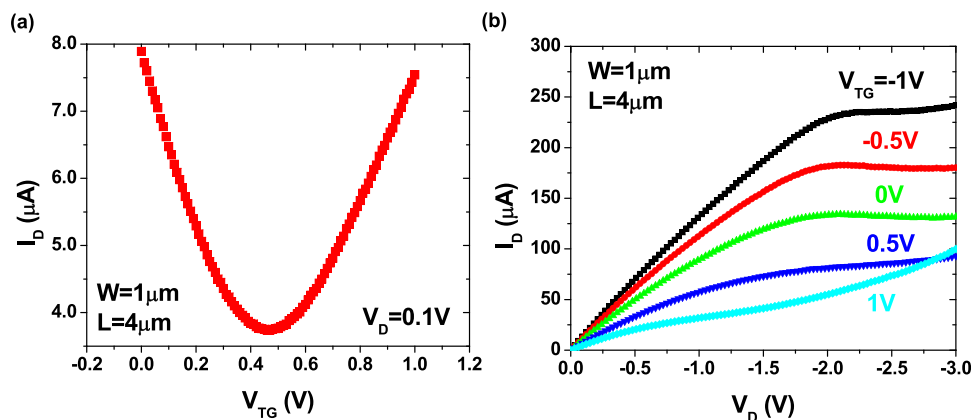

FIG. 2. (a) Drain current as a function of top gate voltage for graphene FET on polyimide with $4\mu m$ gate length. (b) Drain current as a function of drain voltage at various top gate voltage from -1 V to 1 V for graphene FET on polyimide with $4\mu m$ gate length.

and displays the 1/f frequency dependence expected for an ideal FET (Figure 3). In this analysis, a de-embedding procedure is used that takes account of parasitic effects (pad and gate capacitance and resistance). This is done by measuring on-chip inactive "open" and "short" test devices. In the former, there is no graphene in the channel. In the latter, the gate, source, and drain electrodes are all shorted by metal. In Figure 3(a), we show the current gain $|h21|$ as a function of frequency with and without de-embedding ("raw" measurements) for graphene RF device on polyimide with channel length of 400 nm. The cutoff frequency, i.e., the frequency where the current gain becomes unity, is 3 GHz without de-embedding and 10 GHz after de-embedding. To date, this is the highest reported cutoff frequency for graphene transistors on polyimide. This performance is comparable to the graphene on polyethylene naphthalate (PEN) substrates.[17] As compared to PEN substrate, polyimide has the advantage of higher glass transition temperature and higher melting temperature,[30] which opens up more applications in high temperature regime. Organic RF devices on flexible substrates typically operate in the MHz range.[31,32] It is clear from these results that graphene RF devices on polyimide have the advantage of higher operating frequency as compare to organic RF devices. This performance of graphene on polyimide is comparable to those of silicon membranes on flexible substrates,[9] while the graphene on polyimide offers more mechanical flexibility as compared to silicon membrane, which will be discussed next.

The flexibility of the graphene devices on polyimide was investigated. Figure 4(a) shows the drain current I_D as a function of drain voltage V_D for ungated graphene FET

before bending and after bending at radius of 5.9 mm and 1 mm. After each bending, the graphene device was flattened to measure the Id vs V_D. The resistances of the device are extracted from the I_D vs V_D plots. This resistance includes both the channel resistance and contact resistance. Figure 4(b) shows the extracted resistance of the graphene devices after bending the polyimide substrate to various bending radii ranging from flat to 1 mm. The resistance of the graphene devices is stable up to a bending radius as small as 1 mm, indicating excellent mechanical flexibility. This mechanical flexibility is better than that of silicon membranes and III-V membranes on flexible substrates.[9,11]
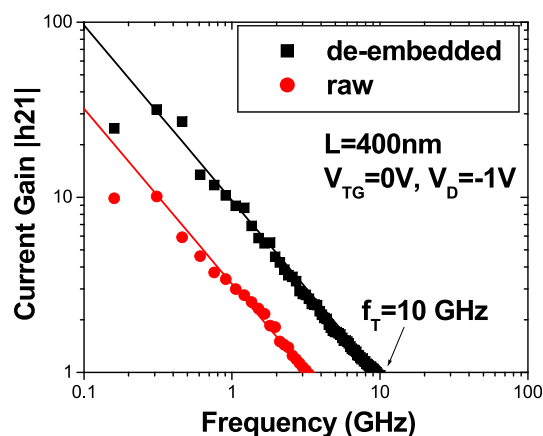

FIG. 3. Small-signal current gain $|h21|$ versus frequency for a 400 nm gate length graphene RF device on polyimide with and without de-embedding. The symbols are measured results and lines are fits. The cut-off frequency after de-embedding is 10 GHz.
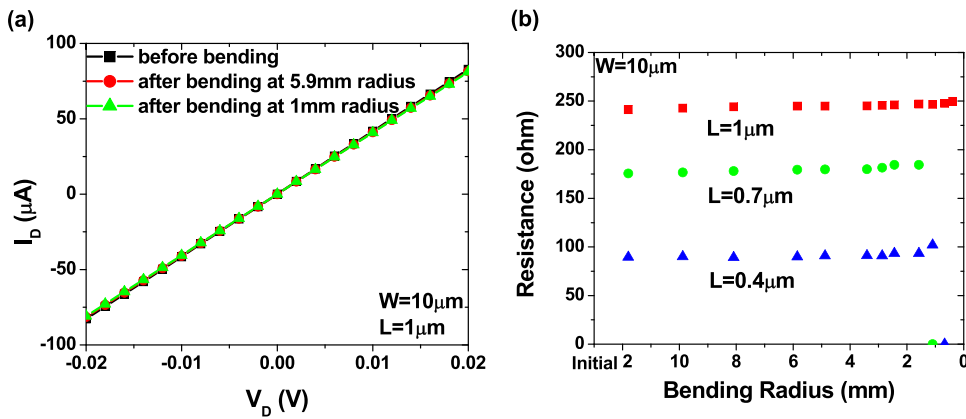
FIG. 4. (a) Drain current as a function of drain voltage for ungated graphene FET with channel length of 1 μm before bending and after bending at 5.9 mm and 1 mm radius. (b) Resistance of the ungated graphene devices as a function of bending radius. The device width is 10 μm. The device lengths are 1 μm, 0.7 μm, and 0.4 μm, respectively.
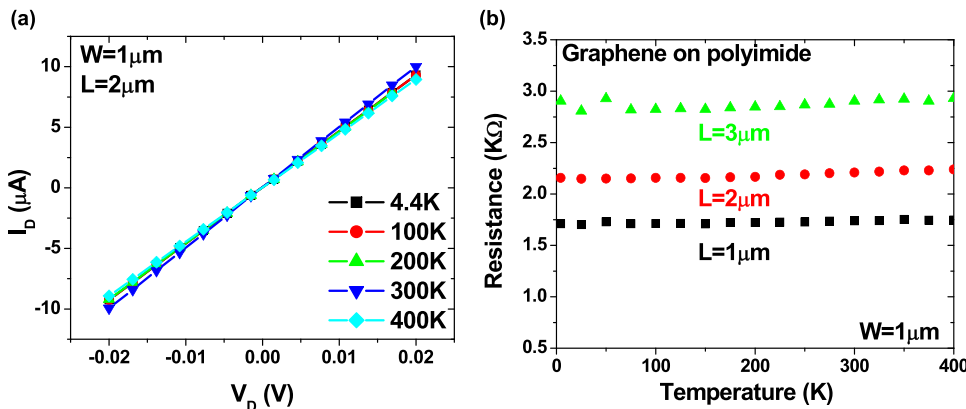

FIG. 5. (a) Drain current as a function of drain voltage for ungated graphene device with 2 μm gate length measured from 4.4 K to 400 K. (b) Temperature dependence of the resistance of the ungated graphene devices on polyimide. The channel length is 1 μm, 2 μm, and 3 μm, respectively.

The temperature stability of the devices was also evaluated. Figure 5(a) shows measured drain current as a function of drain voltage of ungated graphene devices at various temperatures from 4.4 K to 400 K. From the slope of I_D vs V_D plots, the resistance of ungated graphene devices is extracted and plotted as a function of temperature, shown in Figure 5(b). At low temperatures, the dominant scattering mechanism of the carriers is Coulomb scattering by impurities and short-range scattering by defects in exfoliated single layer graphene samples.[33,34] For graphene made by CVD methods, the short-range scattering may be more dominant due to the grain boundaries and other lattice defects formed during the growth and transfer process. The mobility limited by short-range scattering is temperature independent.[33,34] Therefore, the device performances are typically observed as temperature independent for CVD grown graphene.[13,35] At high temperatures, the mobility of graphene on SiO_2/Si substrate usually decrease rapidly, due to the surface optical phonon scattering from SiO_2 substrate.[34,36,37] It has been reported that polyimide buffer layer can effectively reduce phonon scattering.[38] This might be the reason that the channel resistance is unchanged even up to 400 K. This temperature stability implies that the devices may have utility in many harsh environments.

In summary, graphene RF devices have been successfully fabricated on flexible polyimide substrates, and a cutoff frequency as high as 10 GHz has been attained. Excellent channel mobility and current saturation are observed in graphene long channel devices on polyimide. Graphene devices on polyimide exhibit excellent temperature stability and mechanical flexibility.

[1]P. Mach, S. J. Rodriguez, R. Nortrup, P. Wiltzius and J. A. Rogers, Appl. Phys. Lett. **78**(23), 3592–3594 (2001).

[2]S. Bouwstra, L. Feijs, C. Wei and S. B. Oetomo, presented at the Sixth International Workshop on Wearable and Implantable Body Sensor Networks, 2009. BSN 2009.

[3]F. C. Krebs, Sol. Energy Mater. Sol. Cells **93**(4), 394–412 (2009).

[4]J. A. Rogers, Z. Bao, K. Baldwin, A. Dodabalapur, B. Crone, V. R. Raju, V. Kuck, H. Katz, K. Amundson, J. Ewing, and P. Drzaic, Proc. Natl. Acad. Sci. U.S.A. **98**(9), 4835–4840 (2001).

[5]D. H. Kim, N. S. Lu, R. Ma, Y. S. Kim, R. H. Kim, S. D. Wang, J. Wu, S. M. Won, H. Tao, A. Islam, K. J. Yu, T. I. Kim, R. Chowdhury, M. Ying, L. Z. Xu, M. Li, H. J. Chung, H. Keum, M. McCormick, P. Liu, Y. W. Zhang, F. G. Omenetto, Y. G. Huang, T. Coleman, and J. A. Rogers, Science **333**(6044), 838–843 (2011).

[6]L. Teng and W. A. Anderson, IEEE Electron Device Lett. **24**(6), 399–401401 (2003).

[7]M. Mativenga, M. H. Choi, J. W. Choi, and J. Jang, IEEE Electron Device Lett. **32**(2), 170–172 (2011).

[8]H. Sirringhaus, T. Kawase, R. H. Friend, T. Shimoda, M. Inbasekaran, W. Wu, and E. P. Woo, Science **290**(5499), 2123–2126 (2000).

[9]L. Sun, G. X. Qin, J. H. Seo, G. K. Celler, W. D. Zhou, and Z. Q. Ma, Small **6**(22), 2553–2557 (2010).

[10]K. Zhang, J. H. Seo, W. D. Zhou, and Z. Q. Ma, J. Phys. D-Appl. Phys. **45**(14), 116804 (2012).

[11]C. Wang, J.-C. Chien, H. Fang, K. Takei, J. Nah, E. Plis, S. Krishna, A. M. Niknejad, and A. Javey, Nano Lett. **12**(8), 4140–4145 (2012).

[12]Y. Wu, K. A. Jenkins, A. Valdes-Garcia, D. B. Farmer, Y. Zhu, A. A. Bol, C. Dimitrakopoulos, W. Zhu, F. Xia, P. Avouris, and Y.-M. Lin, Nano Lett. **12**(6), 3062–3067 (2012).

[13]Y.-M. Lin, A. Valdes-Garcia, S.-J. Han, D. B. Farmer, I. Meric, Y. Sun, Y. Wu, C. Dimitrakopoulos, A. Grill, P. Avouris, and K. A. Jenkins, Science **332**(6035), 1294–1297 (2011).

[14]H. Wang, A. Hsu, J. Wu, J. Kong, and T. Palacios, IEEE Electron Device Lett. **31**(9), 906–908 (2010).

[15]B. J. Kim, S.-K. Lee, M. S. Kang, J.-H. Ahn, and J. H. Cho, ACS Nano **6**(10), 8646–8651 (2012).

[16]B. J. Kim, H. Jang, S.-K. Lee, B. H. Hong, J.-H. Ahn, and J. H. Cho, Nano Lett. **10**(9), 3464–3466 (2010).

[17]N. Petrone, I. Meric, J. Hone, and K. L. Shepard, Nano Lett. **13**(1), 121–125 (2013).

[18]S. Lee, K. Lee, C.-H. Liu, G. S. Kulkarni, and Z. Zhong, Nat. Commun. **3**, 1018 (2012).

[19]W.-R. Lian, Y.-C. Huang, Y.-A. Liao, K.-L. Wang, L.-J. Li, C.-Y. Su, D.-J. Liaw, K.-R. Lee, and J.-Y. Lai, Macromolecules **44**(24), 9550–9555 (2011).

[20]O. M. Nayfeh, IEEE Electron Device Lett. **32**(10), 1349–1351 (2011).

[21]C. Sire, F. Ardiaca, S. Lepilliet, J. W. T. Seo, M. C. Hersam, G. Darnbrine, H. Happy, and V. Derycke, Nano Lett. **12**(3), 1184–1188 (2012).

[22]S.-K. Lee, B. J. Kim, H. Jang, S. C. Yoon, C. Lee, B. H. Hong, J. A. Rogers, J. H. Cho, and J.-H. Ahn, Nano Lett. **11**(11), 4642–4646 (2011).

[23]S.-K. Lee, H. Y. Jang, S. Jang, E. Choi, B. H. Hong, J. Lee, S. Park, and J.-H. Ahn, Nano Lett. **12**(7), 3472–3476 (2012).

[24]X. Li, W. Cai, J. An, S. Kim, J. Nah, D. Yang, R. Piner, A. Velamakanni, I. Jung, E. Tutuc, S. K. Banerjee, L. Colombo, and R. S. Ruoff, Science **324**(5932), 1312–1314 (2009).

[25]S. Kim, J. Nah, I. Jo, D. Shahrjerdi, L. Colombo, Z. Yao, E. Tutuc, and S. K. Banerjee, Appl. Phys. Lett. **94**(6), 062107 (2009).

[26]D. B. Farmer, A. Valdes-Garcia, C. Dimitrakopoulos, and P. Avouris, Appl. Phys. Lett. **101**(14), 143503 (2012).

[27]C. Kittel, *Introduction to Solid State Physics* (John Wiley and Sons, Inc, 1996).

[28]D. B. Farmer, H.-Y. Chiu, Y.-M. Lin, K. A. Jenkins, F. Xia, and P. Avouris, Nano Lett. **9**(12), 4474–4478 (2009).

[29]J. Zheng, L. Wang, R. Quhe, Q. Liu, H. Li, D. Yu, W.-N. Mei, J. Shi, Z. Gao, and J. Lu, Sci. Rep. **3**, 1314 (2013).

[30]W. A. MacDonald, M. K. Looney, D. MacKerron, R. Eveson, R. Adam, K. Hashimoto, and K. Rakos, J. Soc. Inf. Disp. **15**(12), 1075–1083 (2007).

[31]E. Cantatore, T. C. T. Geuns, G. H. Gelinck, E. van Veenendaal, A. F. A. Gruijthuijsen, L. Schrijnemakers, S. Drews, and D. M. de Leeuw, IEEE Journal of Solid-State Circuits **42**(1), 84–92 (2007).

[32]T. W. Kelley, P. F. Baude, C. Gerlach, D. E. Ender, D. Muyres, M. A. Haase, D. E. Vogel, and S. D. Theiss, Chem. Mater. **16**(23), 4413–4422 (2004).

[33]E. H. Hwang, S. Adam, and S. Das Sarma, Phys. Rev. Lett. **98**(18), 186806 (2007).

[34]W. Zhu, V. Perebeinos, M. Freitag, and P. Avouris, Phys. Rev. B **80**(23), 235402 (2009).

[35]Y. Wu, Y.-m. Lin, A. A. Bol, K. A. Jenkins, F. Xia, D. B. Farmer, Y. Zhu, and P. Avouris, Nature **472**(7341), 74–78 (2011).

[36]J.-H. Chen, C. Jang, S. Xiao, M. Ishigami, and M. S. Fuhrer, Nat. Nanotechnol. **3**(4), 206–209 (2008).

[37]S. Fratini and F. Guinea, Phys. Rev. B **77**(19), 195415 (2008).

[38]T. Taino, M. Yoshida, M. Narisawa, H. Myoren, K. Kikuchi, H. Nakagawa, M. Aoyagi, H. Sato, H. M. Shimizu, and S. Takada, J. Phys.: Conf. Ser. **43**(1), 1319 (2006).